DAMPING IN RING SEALS FOR COMPRESSIBLE FLUIDS

David P. Fleming
National Aeronautics and Space Administration
Lewis Research Center
Cleveland, Ohio 44135

SUMMARY

An analysis is presented to calculate damping in ring seals for a compressible fluid. Results show that damping in tapered ring seals (optimized for stiffness) is less than that in straight bore ring seals for the same minimum clearance. Damping in ring seals can promote fractional frequency whirl and can, thus, be detrimental. Thus, tapered seals can benefit rotor and seal stability by having lower damping as well as higher stiffness. Use of incompressible results leads to large errors.

INTRODUCTION

Ring seals (annular seals) can have a considerable influence on the dynamic behavior of rotors. This is not surprising when one considers that such a seal has the appearance of a journal bearing, although with larger clearances than usual bearing practice. With a large pressure difference across the seal, most of the force generated is due to the high velocity throughflow of sealed fluid. In a series of papers (refs. 1 to 3) Black and coworkers calculated stiffness and damping in annular seals having constant clearance in the axial direction and sealing an incompressible fluid. In references 4 and 5, it was shown that stiffness could be considerably increased by tapering the seal bore so that clearance is greater at the inlet than at the exit. The higher stiffness can be beneficial in stabilizing rotors by shifting critical speeds; floating-ring seals can also benefit from higher stiffness with resulting longer life. Such a tapered bore configuration solved a wear problem in the hot gas seal of the Space Shuttle high pressure oxygen turbopump.

Damping, as well as stiffness, influences seal and rotor behavior. As previously mentioned, damping coefficients were calculated by Black, et al. (refs. 1 to 3), for constant-clearance seals and incompressible fluids. Reference 6 presented damping data for tapered ring seals with incompressible fluids. Heretofore no damping information has been available for seals passing compressible fluids. The purpose of this work is to provide such data for both constant-clearance and tapered seals.

SYMBOLS

B	damping coefficient
$\bar{B}$	dimensionless damping, $BC_2^3/RL^3\mu_0$
$\tilde{B}$	dimensionless damping, $\bar{B}L/Re_0C_2$
C	seal radial clearance
c_v	specific heat at constant volume
e	seal eccentricity
F	seal force
f	Fanning friction factor
g	seal force per unit of circumference, eq. (40)
H	clearance ratio, C_1/C_2
h	seal local film thickness
K	seal stiffness
$\bar{K}$	dimensionless stiffness, KC_2/p_0LD
k	entrance loss coefficient
L	seal length
M	Mach number, $u/\sqrt{\gamma \mathcal{R} T}$
P	pressure ratio, p_t/p_s
p	pressure
Q	M_s^2
q	heat flux
R	seal radius
Re_0	"sonic" Reynolds number, $2\rho_0C_2\sqrt{\gamma \mathcal{R} T_0}/\mu_0$
$\mathcal{R}$	gas constant
T	absolute temperature
t	time

U	velocity ratio, u_t/u_s
u	axial velocity
v	$\partial h/\partial t$
W	Mach number ratio, M_t/M_s
z	axial coordinate
α	seal taper angle
γ	specific heat ratio
ϵ	eccentricity ratio, e/C_2
η	1 + k
θ	circumferential coordinate
μ	dynamic viscosity
ρ	fluid density
υ	density ratio, ρ_t/ρ_s
φ	altitude angle, $\tan^{-1}(B\omega_r/K)$
ω_p	orbital frequency
ω_r	shaft rotational speed

Subscripts:

e	entrance
rad	radial
s	steady state
t	perturbed
tan	tangential
x	seal exit
0	upstream stagnation condition
1	seal entrance
2	seal exit
3	downstream reservoir condition

ANALYSIS

The configuration to be analyzed is that of a tapered bore ring seal whose clearance decreases in the flow direction (fig. 1). Around the circumference the clearance is given by

$$h(z,\theta) = C(z) + C_2\epsilon \cos \theta \tag{1}$$

where C is the clearance when the seal is concentric. The variation of C with axial coordinate z is

$$C(z) = C_1 - \alpha z \tag{2}$$

The analysis is applicable to a straight seal by setting the taper angle α to 0.

When the seal has a velocity relative to the shaft in the radial direction, a damping force is generated. To determine this force, the pressure distribution within the seal will be calculated and integrated over the seal area. The following assumptions are employed:

(1) Eccentricity is small compared with the concentric clearance; that is, $\epsilon \ll 1$.

(2) The fluid behaves as a perfect gas.

(3) Rotational effects on the flow field are neglected; the flow is one-dimensional in the axial direction.

(4) The friction factor is constant everywhere within the seal.

(5) Time derivatives of the fluid properties and velocity are neglected; that is, the flow field is quasi-steady-state. Reference 6 examined this assumption for an incompressible fluid and concluded that acceptable accuracy results.

The analysis begins from the time-dependent equations of continuity, momentum, and energy as presented by Shapiro (ref. 7). For a channel, which the seal passage approximates, these are, respectively,

$$\frac{\partial}{\partial z}(\rho u h) + \frac{\partial}{\partial t}(\rho h) = 0 \tag{3}$$

$$-\frac{\partial}{\partial z}(ph) + p\frac{\partial h}{\partial z} - f\rho u^2 = \frac{\partial}{\partial t}(\rho u h) + \frac{\partial}{\partial z}(\rho u^2 h) \tag{4}$$

$$q = \frac{\partial}{\partial t}\left[\rho h\left(c_v T + \frac{u^2}{2}\right)\right] + \frac{\partial}{\partial z}\left[\rho u h\left(c_v T + \frac{p}{\rho} + \frac{u^2}{2}\right)\right] \tag{5}$$

The momentum equation may be simplified by using the continuity equation. In turn, the energy equation may be simplified through use of the continuity and momentum equations. Additionally, for a perfect gas

$$\frac{p}{\rho} = \mathcal{R}T \tag{6}$$

and

$$c_v = \frac{\mathcal{R}}{\gamma - 1} \tag{7}$$

The seal taper angle is

$$\alpha \equiv \frac{\partial h}{\partial z} \tag{8}$$

Defining

$$v \equiv \frac{\partial h}{\partial t} \tag{9}$$

allows the continuity, momentum, and energy equations to be written as, respectively,

$$\frac{\partial \rho}{\partial t} + \frac{\rho v}{h} + u \frac{\partial \rho}{\partial z} + \rho \frac{\partial u}{\partial z} - \frac{\rho u \alpha}{h} = 0 \tag{10}$$

$$- \frac{\partial p}{\partial z} = \frac{f \rho u^2}{h} + \rho \frac{\partial u}{\partial t} + \rho u \frac{\partial u}{\partial z} \tag{11}$$

$$q/h + \frac{f \rho u^3}{h} + \frac{pv}{h} = \frac{1}{\gamma - 1} \left[\frac{\partial p}{\partial t} + u \frac{\partial p}{\partial z} - \frac{\gamma p}{\rho} \left(\frac{\partial \rho}{\partial t} + u \frac{\partial \rho}{\partial z} \right) \right] \tag{12}$$

The next step is to invoke the small perturbation assumptions and write the pressure, density, and velocity as the sum of a steady-state value plus a small perturbation

$$\left.\begin{aligned} p &= p_s + p_t \\ \rho &= \rho_s + \rho_t \\ u &= u_s + u_t \end{aligned}\right\} \tag{13}$$

The steady-state equations are

$$u_s \frac{d\rho_s}{dz} + \rho_s \frac{du_s}{dz} - \frac{\rho_s u_s \alpha}{h} = 0 \tag{14}$$

$$- \frac{dp_s}{dz} = \frac{f \rho_s u_s^2}{h} + \rho_s u_s \frac{du_s}{dz} \tag{15}$$

$$q_s/h + \frac{f\rho_s u_s^3}{h} = \frac{u_s}{\gamma - 1}\left(\frac{dp_s}{dz} - \frac{\gamma p_s}{\rho_s}\frac{d\rho_s}{dz}\right) \tag{16}$$

The steady-state equations were solved (for $q = 0$) in reference 5 and will not be dealt with further. The perturbed equations of continuity, momentum, and energy are, respectively,

$$\frac{\partial \rho_t}{\partial t} + \frac{\rho_s v}{h} + \frac{\partial}{\partial z}(\rho_t u_s + \rho_s u_t) - \frac{\rho_s u_t \alpha}{h} - \frac{\rho_t u_s \alpha}{h} = 0 \tag{17}$$

$$-\frac{\partial p_t}{\partial z} = \frac{f\rho_t u_s^2}{h} + \frac{2f\rho_s u_s u_t}{h} + \rho_s \frac{\partial u_t}{\partial t} + \rho_s u_s \frac{\partial u_t}{\partial z} + (\rho_s u_t + \rho_t u_s)\frac{\partial u_s}{\partial z} \tag{18}$$

$$q_t/h + \frac{f\rho_t u_s^3}{h} + \frac{3f\rho_s u_t u_s^2}{h} + \frac{p_s v}{h}$$

$$= \frac{1}{\gamma - 1}\left[\frac{\partial p_t}{\partial t} + u_s \frac{\partial p_t}{\partial z} + u_t \frac{\partial p_s}{\partial z} - \frac{\gamma p_t u_s}{\rho_s}\frac{\partial \rho_s}{\partial z} + \frac{\gamma p_s \rho_t u_s}{\rho_s^2}\frac{\partial \rho_s}{\partial z}\right.$$

$$\left. - \frac{\gamma p_s}{\rho_s}\left(\frac{\partial \rho_t}{\partial t} + u_s \frac{\partial \rho_t}{\partial x} + u_t \frac{\partial \rho_s}{\partial z}\right)\right] \tag{19}$$

In accordance with the assumptions, the time derivatives of p_t, ρ_t, and u_t are neglected, and the heat flow q is taken to be zero. Equations (17) to (19) then become ordinary differential equations which may conveniently be written in dimensionless variables

$$\left.\begin{aligned} P &= \frac{p_t}{p_s} \\ \mathfrak{J} &= \frac{\rho_t}{\rho_s} \\ U &= \frac{u_t}{u_s} \end{aligned}\right\} \tag{20}$$

Additionally, the Mach number is defined as

$$M = \frac{u}{\sqrt{\gamma \mathcal{R} T}} = u\sqrt{\frac{\rho}{\gamma p}} \tag{21}$$

As with the other variables, the Mach number may be considered as the sum of a steady-state quantity and a small perturbation.

$$M = M_s + M_t \tag{22}$$

Defining

$$W = \frac{M_t}{M_s} \tag{23}$$

we find, from equation (21),

$$W = U + \frac{\sigma}{2} - \frac{P}{2} \tag{24}$$

After some algebraic manipulation, making use of equations (14) to (16), the perturbed continuity, momentum, and energy equations become, respectively,

$$\frac{d\sigma}{dz} + \frac{dU}{dz} + \frac{v}{u_s h} = 0 \tag{25}$$

$$\frac{dP}{dz} + \gamma Q \frac{dU}{dz} = \frac{2W}{p_s} \frac{dp_s}{dz} \tag{26}$$

$$\frac{dP}{dz} - \gamma \frac{d\sigma}{dz} = \frac{\gamma - 1}{h} \left(2QW\gamma f + \frac{v}{u_s} \right) \tag{27}$$

wherein

$$Q \equiv M_s^2 \tag{28}$$

Thus, we have three simultaneous, ordinary differential equations in four unknown variables P, σ, U, and W. A fourth equation needed to obtain a solution may be obtained by differentiating equation (24) with respect to z:

$$\frac{dW}{dz} = \frac{dU}{dz} + \frac{1}{2} \left(\frac{d\sigma}{dz} - \frac{dP}{dz} \right) \tag{29}$$

Equations (25) to (27) and (29) may now be solved simultaneously for the perturbed variables. As for the steady-state variables (ref. 7), the differential equations for the perturbed variables may be combined to yield a single differential equation in the perturbed Mach number W.

Reference 8 derives a differential equation for the steady-state pressure p_s, which may be written as

$$\frac{1}{p_s} \frac{dp_s}{dz} = - \frac{\gamma Q}{h(1 - Q)} [\alpha + f + f(\gamma - 1)Q] \tag{30}$$

With this, the equation for perturbed Mach number is

$$\frac{dW}{dz} = \frac{W}{h(1 - Q)} \left\{ \frac{(\gamma + 1)Q}{1 - Q} [\alpha + f + f(\gamma - 1)Q] + (\gamma - 1)fQ(\gamma Q + 1) \right\} - \frac{(\gamma + 1)v}{2\gamma u_s h(1 - Q)} \tag{31}$$

From the steady-state solution (ref. 5), Q is a known function of z. Equation (31) will be easier to solve if we make the substitution (ref. 5, eq. (2))

$$\frac{dQ}{dz} = \frac{2Q\left(1 + \frac{\gamma - 1}{2} Q\right)(\gamma fQ + \alpha)}{h(1 - Q)} \tag{32}$$

Also, u_s varies according to (ref. 8)

$$\frac{u_e}{u_s} = \frac{M_e}{M_s} \sqrt{\frac{1 + \frac{\gamma - 1}{2} Q}{1 + \frac{\gamma - 1}{2} Q_e}} \tag{33}$$

where the subscript e denotes the steady-state value at $z = 0$. Equation (31) becomes

$$\frac{dW}{dQ} = \frac{W}{2\left(1 + \frac{\gamma - 1}{2} Q\right)(\gamma fQ + \alpha)} \left[\frac{\gamma + 1}{1 - Q} \alpha + \gamma f \left(\frac{1 + \gamma Q}{1 - Q} + \gamma Q + 1 - Q \right) \right] - \frac{(\gamma + 1)vM_e}{4\gamma u_e Q^{3/2} (\gamma fQ + \alpha) \sqrt{\left(1 + \frac{\gamma - 1}{2} Q\right)\left(1 + \frac{\gamma - 1}{2} Q_e\right)}} \tag{34}$$

The perturbed Mach number W may now be found by solving equation (34).

To determine the seal damping force, the perturbed pressure P must be known. Equations (25) to (27) may be combined to yield a differential equation for P. Making use also of equations (32) and (33) yields

$$\frac{dP}{dQ} = - \frac{\gamma W}{\left(1 + \frac{\gamma - 1}{2} Q\right)(\gamma fQ + \alpha)} \left[\frac{\alpha + \gamma fQ}{1 - Q} + f(1 + \gamma Q - Q) \right] + \frac{vM_e}{2u_e M_s (\gamma fQ + \alpha) \sqrt{\left(1 + \frac{\gamma - 1}{2} Q\right)\left(1 + \frac{\gamma - 1}{2} Q_e\right)}} \tag{35}$$

Boundary conditions. - At the seal exit it is assumed that there is no change in the boundary conditions of the steady-state problem. Thus, for choked flow

$$\left.\begin{aligned} M &= 1 \\ W &= 0 \end{aligned}\right\} \tag{36}$$

For flow which is not choked

$$\left.\begin{aligned} p &= p_3 \\ P &= 0 \end{aligned}\right\} \tag{37}$$

At the seal entrance, the pressure and Mach number are related by (ref. 5)

$$\frac{p}{p_0} = \left(1 + \frac{\gamma - 1}{2}\,\eta Q\right)^{\gamma/(1-\gamma)} \tag{38}$$

The pressure and Mach number may be written as the sums of their steady-state and perturbed components and a binomial expansion performed on the right side of equation (38). After neglecting all powers of Q higher than unity and subtracting out the steady-state terms, there remains

$$P = -\frac{\gamma\eta Q_e W}{1 + \frac{\eta(\gamma - 1)}{2}\,Q_e} \tag{39}$$

Solution of equations. - The results presented herein were obtained through a numerical solution of the differential equations for W and P (eqs. (34) and (35)). For the case of choked flow, $Q = 1$ at the seal exit; it is not possible to integrate numerically to this limit because of the term $1 - Q$ in the denominator of equations (34) and (35). However, W and P may be determined as accurately as desired by taking the solution close to $Q = 1$ without reaching the limit. To ascertain the validity of this approach, equations (34) and (35) may be rewritten, in simplified form, for the case when $Q \to 1$. The resulting equations may be solved analytically, yielding solutions for W and P which remain finite as $Q \to 1$. Thus, the error is of the order $(1 - Q_{lim})P_Q = 1$ which can be made as small as desired by taking Q_{lim} arbitrarily close to 1.

Calculation of seal forces. - The seal force per unit of circumference due to the perturbed pressure p_t is given by

$$g = \int_0^L p_t\,dz = \int_{Q_e}^{Q_x} P p_s \frac{dz}{dQ}\,dQ \tag{40}$$

where Q_x is the value of Q at $z = L$. The steady-state pressure p_s does not contribute to the total seal force because it is uniform around the circumference. From reference 8

$$\frac{p_s}{p_e} = \frac{h_e M_e}{h M_s} \sqrt{\frac{1 + \frac{\gamma - 1}{2} Q_e}{1 + \frac{\gamma - 1}{2} Q}} \tag{41}$$

Making use of this and equation (32) results in

$$g = \frac{1}{2} p_e h_e M_e \sqrt{1 + \frac{\gamma - 1}{2} Q_e} \int_{Q_e}^{Q_x} \frac{P(1 - Q)dQ}{Q^{3/2}\left(1 + \frac{\gamma - 1}{2} Q\right)^{3/2} (\gamma f Q + \alpha)} \tag{42}$$

The integral in equation (42) is easily evaluated numerically.

The total seal damping force in the direction $\theta = 0$ is

$$F = -\int_0^{2\pi} gR \cos \theta \, d\theta \tag{43}$$

For a seal velocity in the direction $\theta = 0$

$$v = v_0 \cos \theta \tag{44}$$

and, thus,

$$g = g_0 \cos \theta \tag{45}$$

where the subscript 0 now denotes the condition at $\theta = 0$. With this the integral in equation (43) may be evaluated, yielding

$$F = -\pi R g_0 \tag{46}$$

A damping coefficient is now defined:

$$B = \frac{F}{v_0} = -\frac{\pi R g_0}{v_0} \tag{47}$$

or

$$B = -\frac{\pi R}{2 v_0} p_e h_e M_e \sqrt{1 + \frac{\gamma - 1}{2} Q_e} \int_{Q_e}^{Q_x} \frac{P(1 - Q)dQ}{Q^{3/2}\left(1 + \frac{\gamma - 1}{2} Q\right)^{3/2} (\gamma f Q + \alpha)} \tag{48}$$

where it is understood that P is evaluated for $v = v_0$. The actual value of v_0 is immaterial. Since both W and P are directly proportional to v_0, it will cancel out of the expressions for the proper choice of dimensionless variables.

RESULTS

The analysis of the preceding section was implemented on a digital computer. The differential equations were solved using a fourth-order Runge-Kutta integrator with automatic error control. The computer programs made use of the results of reference 5.

Results are presented in figures 2 and 3 for choked flow and in figures 4 and 5 for a sealed pressure ratio of 2, for which the flow is not choked. The independent variable in all cases is $Re_0 C_2/L$ where Re_0 is the "sonic" Reynolds number $2C_2\rho_0\sqrt{\gamma \mathcal{R} T_0}/\mu_0$. This independent variable was chosen because laminar flow results are then independent of seal clearance-to-length ratio C_2/L. The specific heat ratio γ was 1.4 for all cases. Results are shown for straight seals and for tapered seals optimized for maximum stiffness-to-leakage ratio (ref. 5).

Figure 2 shows laminar flow results for small values of seal parameter $Re_0 C_2/L$. Damping is plotted in terms of the dimensionless variable

$$\bar{B} = \frac{BC_2^3}{RL^3\mu_0} \tag{49}$$

There is little variation for the range of seal parameter up to 10. Damping approaches a constant value as $Re_0 C_2/C \to 0$. Damping is higher in the straight seal than in the tapered design because of the lower average clearance (seals are compared on the basis of minimum clearance).

Figure 3 shows results for choked flow over the complete range of seal parameter for both laminar and turbulent flow. In this figure, damping is shown in terms of the dimensionless quantity

$$\tilde{B} = \frac{\bar{B}L}{Re_0 C_2} = \frac{BC_2}{2RL^2\sqrt{\gamma P_0 \rho_0}} \tag{50}$$

For this choice of variable, laminar flow damping varies strongly with seal parameter. In contrast, turbulent flow damping shows a much smaller variation. For turbulent flow, damping depends on clearance-to-length ratio C_2/L, appearing to reach a minimum for the middle values of C_2/L investigated, and rising for either higher or lower values. Overall, however, variation is small even for the extreme values of C_2/L considered; thus, for all other factors held constant, equation (50) indicates that damping is approximately proportional to the square of seal length.

The left end of the curves for turbulent flow corresponds to a Reynolds number in the seal passage of 3000; this is generally considered the lowest value for which one can be assured of turbulent flow. A Reynolds number of 2300 is usually taken as the upper limit for laminar flow. Points where Re = 2300 are shown for various C_2/L values on the laminar flow curves.

Damping for a pressure ratio of 2 is shown in figure 4 for small values of Re_0C_2/L. For this pressure ratio the flow is not choked. In common with figure 2, damping does not vary greatly with seal parameter.

Results for a pressure ratio of 2 are shown in figure 5 for the complete range of seal parameter. As in figure 3, the damping is expressed as

$$\tilde{B} = \frac{BC_2}{2RL^2\sqrt{\gamma P_0 \rho_0}}$$

For the straight seal, damping values are lower than for choked flow, as less mass passes through the seal when the flow is unchoked. For the tapered seal, damping for $p_0/p_3 = 2$ is higher than the choked case when the flow is laminar and somewhat lower when the flow is turbulent. This apparently anomalous behavior for laminar flow can be explained by observing that the optimum clearance ratio is lower for $p_0/p_3 = 2$ than for choked flow; thus, the average clearance is less than in the seal optimized for choked flow. Optimum clearance ratios $H = C_1/C_2$ appear in figures 6 and 7 (taken from ref. 5).

Example of seal calculation. - Calculate damping for the example seal of reference 5. Pertinent seal data are

$L = 10$ mm

$D = 50$ mm

$C_2 = 0.05$ mm

$p_0 = 100$ bar

$p_3 = 4$ bar

$T_0 = 800$ K

Fluid: Hydrogen gas

Thus, it was calculated in reference 5 that

$$\frac{C_2}{L} = 0.005$$

$$Re_0 = 37\ 100$$

$$Re_0 \frac{C_2}{L} = 186$$

The flow is choked; thus, damping data are taken from figure 3. For a straight seal

$$\tilde{B} = 0.89$$

yielding

$$B = 570 \text{ N sec/m}$$

For the tapered seal

$$\tilde{B} = 0.47$$

and

$$B = 300 \text{ N sec/m}$$

Effect of seal rotation. - The effect of rotation was examined in reference 6 for a seal passing incompressible fluid using an approximation derived by Black and Jenssen (ref. 2). For the analysis presented herein, fluid temporal derivatives were neglected; thus, the inertia terms calculated in reference 6 do not appear in the present results. The expression for seal forces then becomes

$$\begin{bmatrix} F_x \\ F_y \end{bmatrix} = - \begin{bmatrix} K & \frac{1}{2} B\omega_r \\ -\frac{1}{2} B\omega_r & K \end{bmatrix} \begin{bmatrix} x \\ y \end{bmatrix} - \begin{bmatrix} B & 0 \\ 0 & B \end{bmatrix} \begin{bmatrix} \dot{x} \\ \dot{y} \end{bmatrix} \tag{51}$$

In equation (51) ω_r is the shaft rotational speed.

In the usual case of seal motion, the seal journal describes some orbit within the seal clearance. We will consider the case of a centered circular orbit with orbital frequency ω_p. For this condition, it is easy to calculate the radial restoring force and the tangential (whirl direction) force. Similar to reference 6, we find

$$\left.\begin{aligned} F_{rad} &= -Ke \\ F_{tan} &= Be\left(\frac{1}{2}\omega_r - \omega_p\right) \end{aligned}\right\} \tag{52}$$

where e is the eccentricity of the seal (fig. 8). The radial force depends only on the eccentricity e (the minus sign appears because F_{rad} is defined as positive in the outward direction). The tangential force, however, depends on the relative magnitudes of the spin and whirl speeds. Equation (52) may be written in terms of radial and tangential stiffnesses:

$$\left.\begin{aligned} K_{rad} &= -\frac{F_{rad}}{e} = K \\ K_{tan} &= -\frac{F_{tan}}{e} = -B\omega_r\left(\frac{1}{2} - \frac{\omega_p}{\omega_r}\right) \end{aligned}\right\} \tag{53}$$

A positive value of K_{tan} will inhibit positive whirl; conversely, negative K_{tan} promotes positive whirl. Equation (53) for K_{tan} shows that a positive damping coefficient promotes forward whirl when $\omega_p/\omega_r < 1/2$ and inhibits whirl when $\omega_p/\omega_r > 1/2$. As pointed out in reference 6, this is remarkably similar to the behavior of a full circular journal bearing. The seal differs from a self-acting bearing (but is similar to an externally pressurized bearing) in

that the radial stiffness is independent of whirl speed. Equation (53) also shows that damping in a rotating seal is not entirely beneficial. Damping produces a tangential force which inhibits synchronous whirl but promotes whirl at half frequency or less.

Example of whirl forces. - Seal damping has been presented in dimensionless form, as were stiffness and leakage in reference 6. Also, damping force varies with rotor speed (eq. (53)). Thus, the relative size of the radial and tangential stiffness of equation (53) can only be compared for specific examples. The seal example above is similar to one of the hot-gas seals in the Space Shuttle high-pressure oxygen turbopump. This pump has a nominal operating speed of 31 000 rpm at full-power level. For this speed, table I compares the stiffness and damping for straight and tapered seals. Stiffness data are taken from reference 6. As table I shows, tapered seal stiffness is much higher than that for a straight seal, and damping lower. This means that for a tapered seal the force generated is more nearly in line with the displacement, a situation that is considered to promote stability.

Difference between compressible and incompressible results. - Before the availability of stiffness, damping, and leakage flow data for seals handling compressible fluids, some workers used incompressible data as the "best available." It is instructive to examine the difference in results using compressible and incompressible analyses. Table II compares results for the seal used in the example above. Compressible fluid stiffness and leakage flow are taken from reference 5. Incompressible data from references 4 and 6 are applied two ways: first using the upstream (stagnation) fluid density and second using fluid density as the mean of upstream and downstream densities.

The incompressible theory grossly overestimates seal stiffness, by an order of magnitude for the straight seal. There is little difference in using upstream or mean density. Damping is underestimated by the incompressible theory more severely when the mean density is used. Leakage flow is overestimated by incompressible theory, although not as much when a mean density is used.

One would not expect incompressible theory to yield accurate results because the nature of the flow is much different than with a compressible fluid. Fluid compressibility results in decreasing density and increasing velocity in the flow direction, and the flow becomes choked for large pressure ratios. The pressure gradient increases in the flow direction and, theoretically, becomes infinite at the seal exit for choked flow.

CONCLUDING REMARKS

An analysis has been performed to calculate the damping in straight and tapered seals for a compressible fluid. Results show that damping in optimized tapered seals is considerably less than in straight seals for the same minimum clearance. It was also pointed out that damping in rotating seals is not entirely beneficial as it can sometimes promote whirl. Thus, for rotor or seal

stabilization, tapered seals may confer a double benefit. Not only is tapered seal stiffness generally higher than that for straight seals, but damping is lower.

REFERENCES

1. Black, H. F.: Effects of Hydraulic Forces in Annular Pressure Seals on the Vibrations of Centrifugal Pump Rotors. J. Mech. Eng. Sci., vol. 11, no. 2, Apr. 1969, pp. 206-213.

2. Black, H. F.; and Jenssen, D. N.: Dynamic Hybrid Bearing Characteristics of Annular Controlled Leakage Seals. Proc. Inst. Mech. Eng., vol. 184, part 3N, 1969-70, pp. 92-100.

3. Black, H. F.; and Jenssen, D. N.: Effects of High Pressure Ring Seals on Pump Rotor Vibrations. ASME Paper 71-WA/FE-38, 1971.

4. Fleming, D. P.: High Stiffness Seals for Rotor Critical Speed Control. ASME Paper 71-DET-10, Sep. 1977.

5. Fleming, D. P.: Stiffness of Straight and Tapered Annular Gas Path Seals. J. Lubr. Technol., vol. 101, no. 3, July 1979, pp. 349-355.

6. Fleming, D. P.: Damping in Tapered Annular Seals for an Incompressible Fluid. NASA TP-1646, 1980.

7. Shapiro, A. H.: The Dynamics and Thermodynamics of Compressible Fluid Flow, Vol. II. Ronald Press Co., 1953.

8. Zuk, J.; and Smith, P. J.: Computer Program for Quasi-One-Dimensional Compressible Flow with Area Change and Friction - Application to Gas Film Seals. NASA TN D-7481, 1974.

TABLE I. - STIFFNESS AND DAMPING FOR HPOTP

STRAIGHT AND TAPERED SEALS

	Straight seal	Tapered seal
Dimensionless stiffness, $\bar{K}$	0.015	0.095
Stiffness, K, MN/m	1.5	9.5
Dimensionless damping, $\tilde{B}$	0.89	0.47
Damping, B, N sec/m	570	300
$B\omega_r$, MN/m	1.9	1.0
Attitude angle φ, deg	51	6

TABLE II. - COMPARISON OF COMPRESSIBLE AND INCOMPRESSIBLE RESULTS FOR

HPOTP STRAIGHT AND TAPERED SEALS

	Stiffness, K, MN/m		Damping, B, N sec/m		Leakage flow, g/sec	
	Straight seal	Tapered seal	Straight seal	Tapered seal	Straight seal	Tapered seal
Compressible theory	1.5	9.5	570	300	17	22
Incompressible theory, stagnation density	15.1	29.1	308	245	32	42
Incompressible theory, mean density	14.6	28.6	223	176	22	29

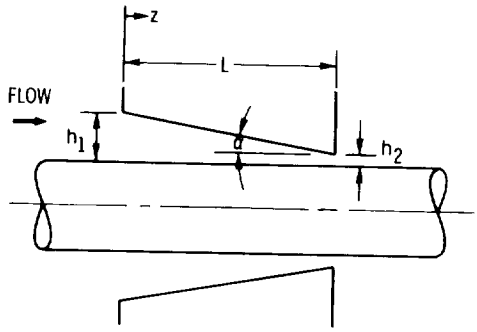

Figure 1. - Tapered ring seal.

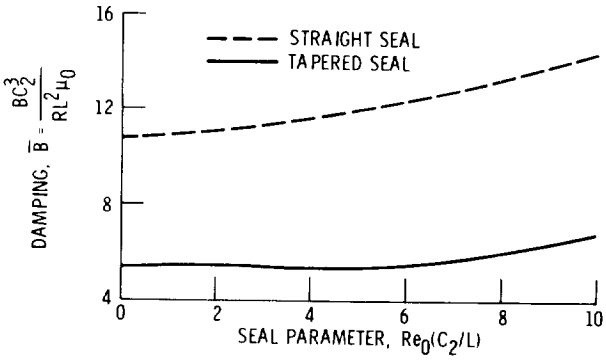

Figure 2. - Damping in ring seals; choked, laminar flow, small value of seal parameter.

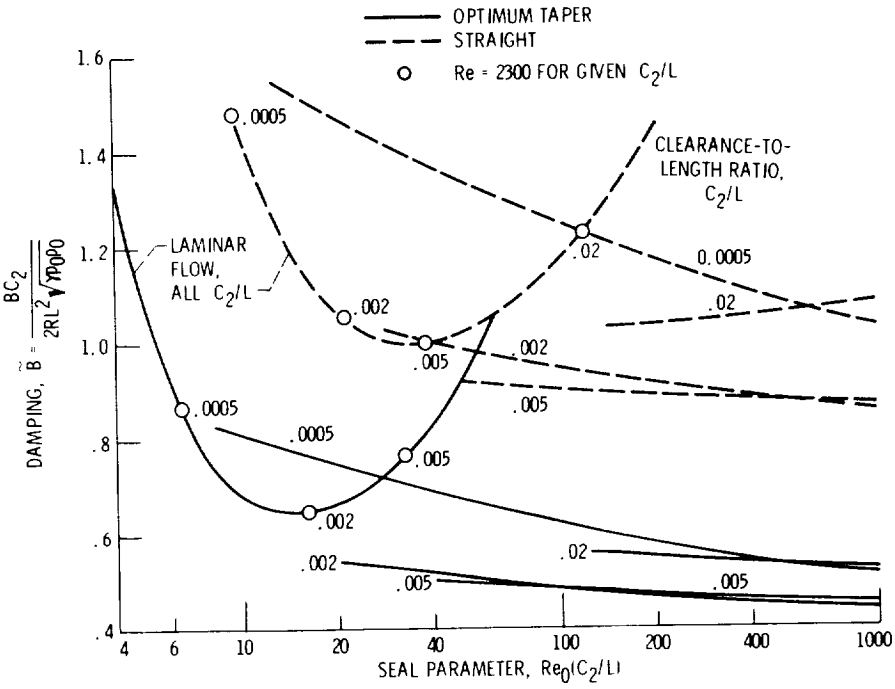

Figure 3. - Damping in ring seals; choked flow, laminar and turbulent.

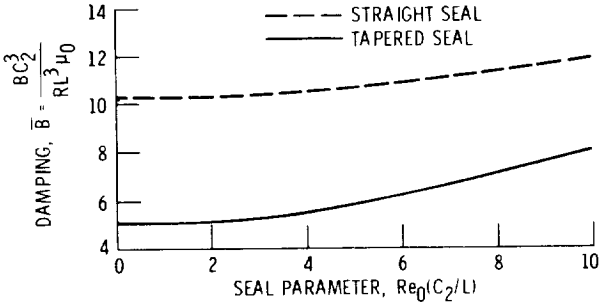

Figure 4. - Damping in ring seals; unchoked, $p_0/p_3 = 2$, laminar flow, small values of seal parameter.

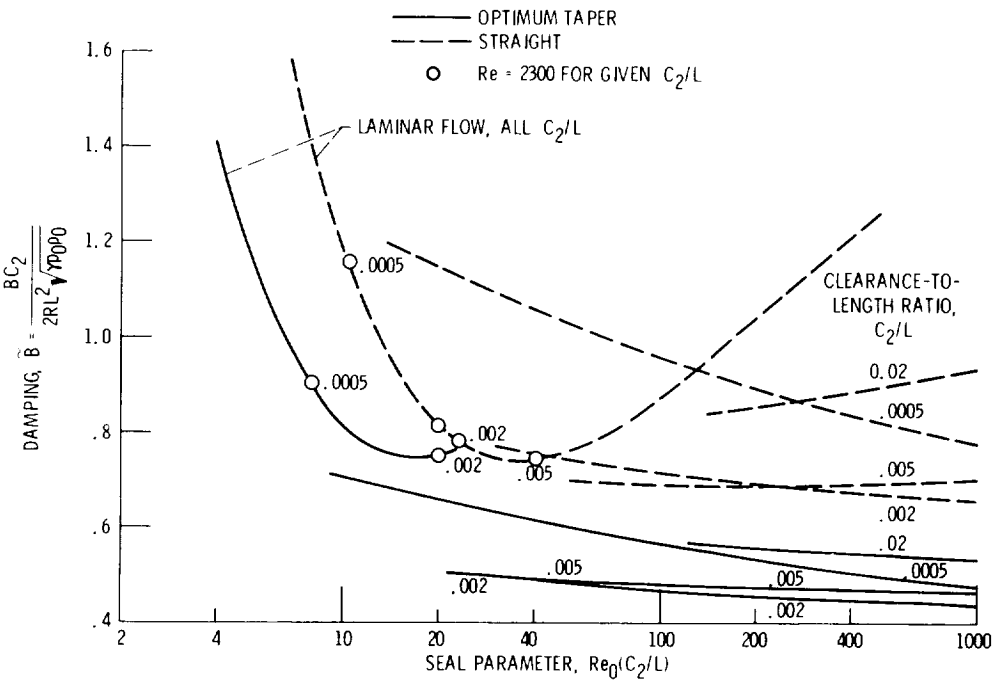

Figure 5. - Damping in ring seals; $p_0/p_3 = 2$, laminar and turbulent flow.

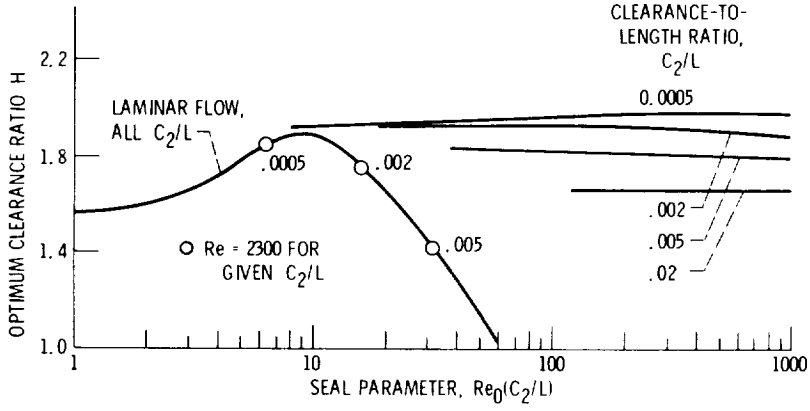

Figure 6. - Optimum clearance ratio of tapered seals, choked flow.

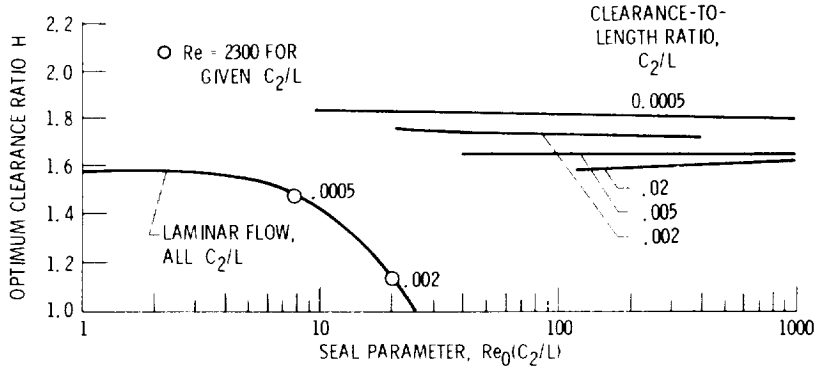

Figure 7. - Optimum clearance ratio of tapered seals, unchoked ($p_0/p_3 = 2$) flow.

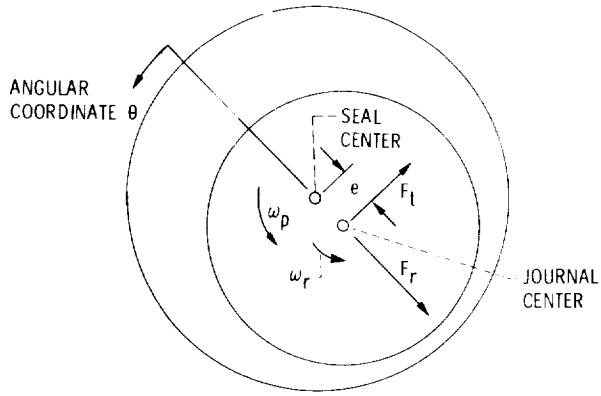

Figure 8. - Whirling seal.